Holistic discretisation illuminates and enhances the numerical modelling of differential equations

A. J. ROBERTS
Department of Mathematics and Computing
University of Southern Queensland
Toowoomba, Queensland 4350
AUSTRALIA

Abstract: I give an overview of some recent developments in using modern dynamical systems theory to derive numerical discretisations of dissipative partial differential equations. The approach provides a systematic way of deriving robust and accurate numerical models. This arises because the method automatically parametrises subgrid scale processes. Good performance at finite grid size should greatly decrease the cost of numerical simulations. Further, it is straightforward both to incorporate boundary conditions on the edges of the domain and to provide initial conditions for forecasting. By making minor modifications of computer algebra programs others may readily apply these methods to their own numerical approximation problems.

Key-Words: subgrid structure, finite elements, numerical discretisation, dynamical systems, initial conditions, boundary conditions, centre manifold theory

1 Introduction

In the western Pacific ocean two dynamically active broad layers have been identified as shown schematically in Fig. 1—to model their evolution we might suppose the interaction between the layers is weak (§2). *The same assumption works generally* to form the basis of numerical discretisations of partial differential equations (PDEs): we slice the domain into finite sized elements by *initially* artificially insulating them from each other (§3); then centre manifold theory [1, 2, e.g.] is applied (§4) to generate a discretisation that incorporates the actual coupling between the elements.

There are manyfold benefits of this dynamical systems approach: in §4 we see it gives new theoretical support for use of the discretisation at finite element size [22]; in practise this comes from resolving subgrid scale structures (§4) and subgrid interactions between physical processes [21, 12]; which generally improves the stability properties of the discretisation [22, 11] and also promotes the use of relatively large grid spacing; the numerical model may be systematically refined, see §5, to higher order consistency and to include more subgrid interactions; boundary conditions on the edges of the domain are straightforwardly incorporated into the same methodology §6 [20]; whereas §8 illuminates the initial conditions needed to ensure long term accuracy [23, 19]; and in §9 the same modelling paradigm, namely centre manifold theory, is used for both numerical and analytic models.

The approach proposed here is based purely upon the *local* dynamics on small elements while maintaining, as do inertial manifolds [27, e.g.], fidelity with the solutions of the original dissipative PDE across the whole domain. Here the analysis rests upon the exponential decay of the small, subgrid structures in each local element, whereas the inertial manifold approach seeks to construct global models [16, 4, 13, e.g.]. One favourable consequence is that here there is no need to invoke a highly restrictive spectral gap condition [7, Eqn. (5.4) e.g.]. The nonlinear Galerkin method, though appealing and though improving convergence [10, e.g.], is impractical in applications with possibly varying coefficients and complicated boundaries. Here I overview recent developments in an immensely inter-

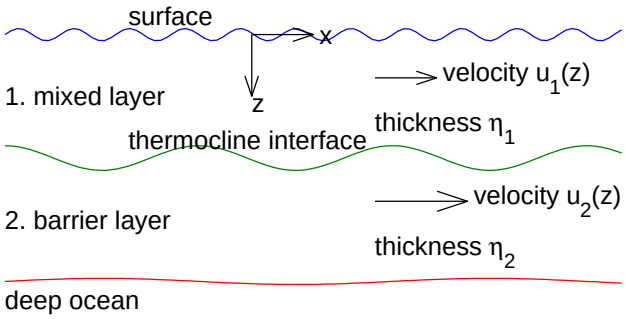

Figure 1: schematic diagram of the mixed layer and the barrier layer above a deep ocean: the main quantities of interest are the thickness of each layer, η_j, and the mean velocity in each layer, $\bar{u}_j$.

esting innovation in the application of dynamical systems theory to the construction of element based discretisations for numerical solution.

2 Two layers in the ocean suggest the approach

Two identifiable layers, drawn in Fig. 1, can survive near the surface of the western Pacific ocean by supposing there is little mixing between the layers. Density jumps do limit turbulent mixing. The mathematical expression of the ideal case of no mixing is to "insulate" the layers from each other:

$$\frac{\partial u_1}{\partial z} = \frac{\partial u_2}{\partial z} = 0 \quad \text{at the interface.}$$

But we actually want a limited interaction between layers, say proportional to the velocity difference as the faster layer drags the slower somewhat:

$$\frac{\partial u_1}{\partial z} = \frac{\partial u_2}{\partial z} = \gamma(u_2 - u_1)\,, \tag{1}$$

where γ parametrises the interlayer coupling. Such interlayer coupling must be *small in effect* to reflect that two identifiable layers exist.

Herein we discuss how the same idea of introducing an artificial coupling between adjacent elements may be applied quite generally. However, for the sake of a clear exposition we consider primarily the well known Burgers' equation [21] for a scalar field $u(x\,,t)$

$$\frac{\partial u}{\partial t} = \frac{\partial^2 u}{\partial x^2} - u\frac{\partial u}{\partial x}\,, \tag{2}$$

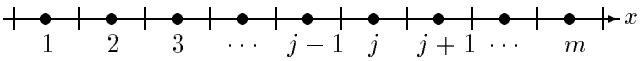

Figure 2: divide the domain into m elements of width h by introducing artificial internal boundary conditions and place grid points in the middle of each element.

which combines the core physical processes of dissipation and nonlinear advection. (The same analysis works for other dissipative PDEs such as the Kuramoto-Sivashinsky equation [12].) A standard finite difference approximation in x is

$$\begin{aligned}\frac{\partial u_j}{\partial t} &= \frac{1}{h^2}\left(u_{j+1} - 2u_j + u_{j-1}\right) \\ &\quad - \frac{1}{2h}u_j\left(u_{j+1} - u_{j-1}\right)\,,\end{aligned} \tag{3}$$

to form a semi-discrete scheme [5, 7, e.g.] for $u_j(t)$, the grid value of u on a spatial grid with spacing h. But other discretisations of the nonlinear term are also consistent with Burgers' equation [8, 5, e.g.]. For example, we could equally as consistently approximate the nonlinear terms as

$$u\frac{\partial u}{\partial z} = \frac{\partial}{\partial x}\left(\tfrac{1}{2}u^2\right) \approx \frac{1}{4h}\left(u_{j+1}^2 - u_{j-1}^2\right)\,.$$

A challenge is to decide *which should be used.*

The answer deduced in our dynamical systems approach [21] is to nonlinearly enhance the dissipation! Specifically

$$\begin{aligned}\frac{\partial u_j}{\partial t} &= \frac{1}{h^2}\left(1 + \frac{h^2}{12}u_j^2\right)\left(u_{j+1} - 2u_j + u_{j-1}\right) \\ &\quad - \frac{1}{2h}u_j\left(u_{j+1} - u_{j-1}\right)\,.\end{aligned} \tag{4}$$

We may also view this change as using upwind differences for the advection term. Either interpretation is well recognised as improving the stability of the discretisation.

3 Slice the domain into finite elements

Suppose we wish to numerically solve for a field $u(x\,,t)$ on some domain. Divide the domain into m finite elements (of size h) as shown in Fig. 2. This is done

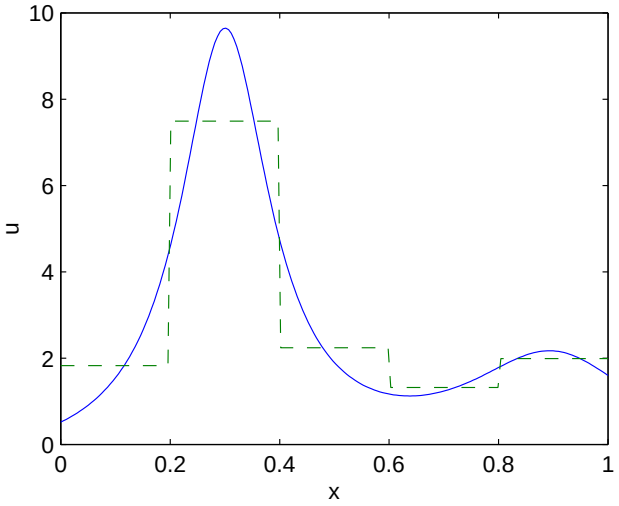

Figure 3: a domain divided into five elements, $h = 0.2$, by insulating IBCs. After transients decaying like $\exp(-t\pi^2/h^2)$, the initial field (solid) would evolve to be constant in each element (dashed).

by introducing the following artificial internal boundary conditions (IBCs) similar to (1):

$$\frac{\partial u^+}{\partial x} - \frac{\partial u^-}{\partial x} = 0 \quad \text{and} \tag{5}$$

$$(1-\gamma)\frac{h}{2}\left(\frac{\partial u^+}{\partial x} + \frac{\partial u^-}{\partial x}\right) = \gamma(u^+ - u^-)\,, \tag{6}$$

where $u^\pm$ denotes the field just to the right/left of an internal boundary:

- when the coupling parameter $\gamma = 0$ the right-hand sides vanish and these IBCs reduce to the insulating conditions $u^\pm_x = 0$;
- whereas when $\gamma = 1$ these IBCs require continuity of the field and its derivative to ensure that the PDE, here Burgers' equation (2), is satisfied throughout the domain.

Linearly, $u_t = u_{xx}$, and in the absence of interelement coupling, $\gamma = 0$, the diffusion acts independently within each element to cause any initial field to decay to a constant in each element as shown schematically in Fig. 3. The constant in each element is independent of the other elements (linearly it only depends upon the initial field in each element). This decay occurs rapidly, on a time scale of h^2/π^2. Thus, exponentially quickly the system settles into a state parametrised by m grid values, each characterising the field in each element.

With interelement coupling, $\gamma \neq 0$, and in the presence of nonlinearities, the field will evolve as "information" flows between elements. However, the diffusive decay in each element causes the field to be still parametrised by the m grid values u_j. For example, we find [21] that for Burgers' equation (2) the field

$$\begin{aligned} u &= u_j + \gamma\left[\mu\delta u_j\,\xi + \tfrac{1}{2}\delta^2 u_j\,\xi^2\right] \\ &\quad + \gamma h u_j \delta^2 u_j\left(\tfrac{1}{6}\xi^3 - \tfrac{1}{8}\xi\right) \\ &\quad + \gamma h^2 u_j^2 \delta^2 u_j\left(\tfrac{1}{24}\xi^4 - \tfrac{1}{48}\xi^2\right) + \mathcal{O}(\|u\|^4, \gamma^2)\,, \end{aligned} \tag{7}$$

where $\xi = (x - x_j)/h$ is an element based coordinate and I have used centred difference and mean operators, $\delta u_j = u_{j+1/2} - u_{j-1/2}$ and $\mu u_j = \frac{1}{2}(u_{j+1/2} + u_{j-1/2})$ respectively. To parametrise the evolving field, these grid values evolve according to some prescription, such as (3) or (4). These form numerical models for the dynamics. We proceed to derive them by a perturbative analysis in nonlinearity and the strength of the interelement coupling γ; the analysis is based upon the uncoupled linear exponential collapse shown in Fig. 3, but accounts for the consequently generated subgrid scale fields such as (7).

4 Centre manifold theory assures fidelity

Centre manifold theory [1, 2, e.g.] addresses the dynamics of perturbed dynamical systems. Applied to Burgers' equation (2) with IBCs (5–6) and based upon the linear picture of the previous section the theory guarantees three things:

existence, there exists an m-dimensional model, composed of actual solutions of the PDE as indicated in Fig. 4, parametrised by the m grid values u_j (one for each element) and the interelement coupling γ:

$$u(x,t) = v(\boldsymbol{u}, x, \gamma) \quad \text{s.t.} \quad \dot{u_j} = g_j(\boldsymbol{u}, \gamma)\,, \tag{8}$$

where $\boldsymbol{u} = (u_1, \ldots, u_m)$;

relevance, the model is exponentially quickly attractive to *all* nearby solutions of the PDE (sometimes called asymptotic completeness [24, e.g.] or exponential tracking [6, e.g.]) so we are assured that

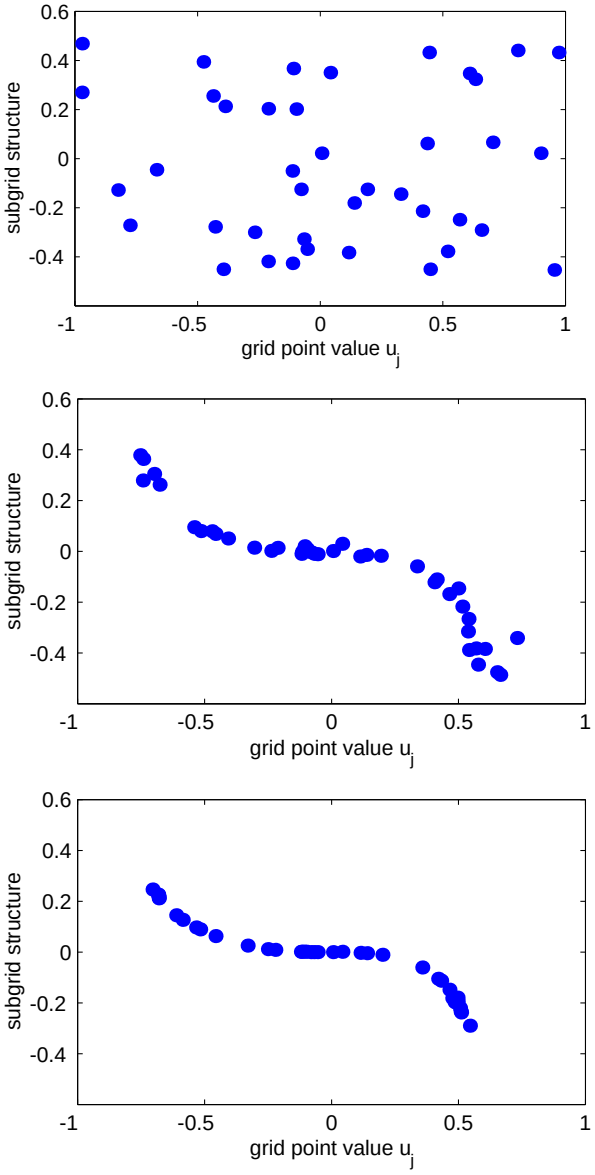

Figure 4: schematic dynamical system view of the evolution in $m = 40$ elements plotting the grid value u_j horizontally and a measure of the subgrid structure vertically. Starting (top) from some random initial condition; after three decay times (middle) almost all elements have collapsed onto a state where the subgrid field is simply parametrised by the grid values; and soon after (bottom) they just evolve along the centre manifold.

the solutions of the model represent the dynamics from a complete range of initial fields, as demonstrated in Fig. 4;

approximation, to construct the model it is appropriate to substitute the above ansatz (8) and solve asymptotically whence the model has the same order of error as the residuals of the governing equations.

Impressively, these properties all hold for *finite grid size* h—there is no need to invoke small h in this approach. The only caveat to these amazingly strong results for the numerical model at finite h is that they apply to some neighbourhood of small $(\boldsymbol{u}, \gamma)$, whereas we have to use the discretisation at finite u_j and for interelement coupling $\gamma = 1$. We hope that the neighbourhood of applicability includes these relevant parameter values; in [21, §A] I showed convergence when evaluated at $\gamma = 1$ for periodic solutions to Burgers' equation. There are as yet unresolved issues about how reliable these assurances are in general. See §5 for more discussion about the new implications of the support this theory gives numerical models.

The construction of the numerical model resolves subgrid scale processes. A practical method to find the centre manifold and the evolution thereon is to substitute an approximate ansatz (8) into the governing PDE, here Burgers' equation (2), and iteratively refine (8). Such an iterative algorithm using computer algebra is described in [18]. Successive iterations involve solving for corrections v' and g' in each element the underlying linear problem of the PDE: here the diffusion problem

$$\frac{\partial^2 v'}{\partial x^2} = g' + \text{PDE residual}(\boldsymbol{u}, x, \gamma) \,, \qquad (9)$$

forced by the residual of the PDE and the IBCs. Thus in the process of forming the numerical model we construct a detailed picture of the subgrid processes. For Burgers' equation (2) we determine the subgrid field (7) in [21]. These resolved subgrid structures are not imposed arbitrarily upon the solution field, but are a natural consequence of the physical dynamics expressed in the PDE through the interelement coupling. It is for this reason I call the model a "holistic discretisation".

Associated with the subgrid fields (7) of the centre manifold is the corresponding evolution

$$\frac{\partial u_j}{\partial t} = \frac{\gamma}{h^2}\left(1 + \frac{h^2}{12}u_j^2\right)\delta^2 u_j - \frac{\gamma}{h}u_j \mu\delta u_j$$

$$+ \mathcal{O}(\|\boldsymbol{u}\|^4, \gamma^2)\,. \qquad (10)$$

Evaluating at $\gamma = 1$ we recover the discretisation (4) for Burgers' equation (2). Such a model has good nonlinear behaviour, as reported in [21], because of the resolution of subgrid scale processes.

5 High order consistent approximations

To date I have only presented formula with γ^1 terms. By, for example, determining γ^2 terms we would obtain a numerical discretisation of bandwidth 5 in the index j. This allows us to develop higher order representations of the spatial derivatives in a PDE.

The IBCs (5–6) may be changed in detail and still behave usefully for interelement coupling γ ranging from 0 to 1. We may use this freedom to force the discretisations to satisfy additional properties. Thus I have *additionally* sought high order consistency as grid size $h \to 0$ using specially crafted IBCs. In [22] I proved that the following nonlocal IBCs ensure consistency to all orders for general linear PDEs:

$$\underbrace{v_j(\boldsymbol{u}, x_{j\pm1}, \gamma) - v_j(\boldsymbol{u}, x_j, \gamma)}_{\approx \pm h \frac{\partial v_j}{\partial x} \text{ at } x = x_j \pm h/2} = \gamma(u_{j\pm1} - u_j)\,, \qquad (11)$$

where $v_j(\boldsymbol{u}, x, \gamma)$ denotes the field of the centre manifold in the jth element. Application to various PDEs have shown that these IBCs generate high order consistency for the nonlinear terms as well. For example, for Burgers' equation (2) the following numerical model is obtained [20] by retaining γ^2 terms:

$$\begin{aligned}
\frac{\partial u_j}{\partial t} &= \frac{1}{h^2}\left[\gamma\delta^2 u_j - \frac{\gamma^2}{12}\delta^4 u_j\right] \\
&- \frac{1}{h}u_j\left[\gamma\mu\delta u_j - \frac{\gamma^2}{6}\mu\delta^3 u_j\right] \\
&+ \frac{\gamma^2}{24h}(\delta^2 u_j\,\mu\delta^3 u_j + \delta^4 u_j\,\mu\delta u_j) \\
&+ \frac{\gamma(1-\gamma)}{12}u_j^2\delta^2 u_j - \frac{\gamma^2}{30}u_j^2\delta^4 u_j \\
&- \frac{\gamma^2}{1440}u_j\left[25\delta^2 u_j\,\delta^4 u_j + 100\mu\delta u_j\,\mu\delta^3 u_j\right. \\
&\quad \left. + 36(\delta^2 u_j)^2\right] \\
&- \frac{\gamma^2}{576}\left[8\delta^2 u_j\,\mu\delta u_j\,(\mu\delta u_j + \mu\delta^3 u_j) + 2(\delta^2 u_j)^3\right. \\
&\quad \left. + \delta^4 u_j\,(4(\mu\delta u_j)^2 + (\delta^2 u_j)^2)\right] \\
&+ \mathcal{O}(\|\boldsymbol{u}\|^4, \gamma^3)\,. \qquad (12)
\end{aligned}$$

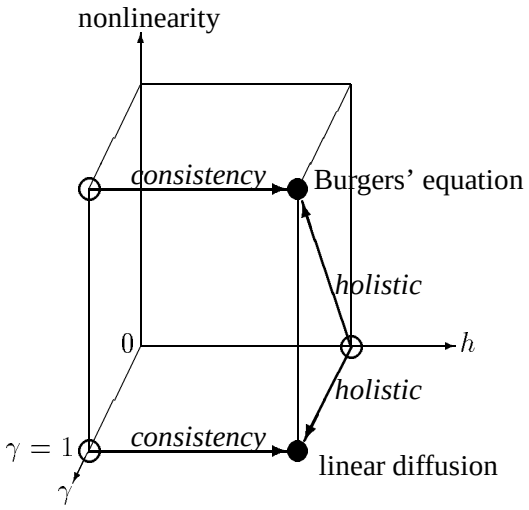

Figure 5: conceptual diagram showing that with the discrete IBCs (11) the numerical model is supported by two independent bases: from $h = 0$ and from $\gamma = 0$.

See that when $\gamma = 1$: the first two lines are $\mathcal{O}(h^4)$ direct approximations of Burgers' equation (2); the third line modifies the nonlinear advection; the fourth lines cancels the nonlinearly enhanced diffusion which appears at $\mathcal{O}(\gamma)$ and replaces it with a nonlinearly enhanced fourth order dissipation; and the remaining lines account for subtle effects of nonlinear subgrid scale evolution, advection and diffusion. This discretisation is fourth order consistent with Burgers' equation as $h \to 0$ [20].

I summarise the new view of numerical discretisations given by this approach as so far established. As shown schematically in Fig. 5, employing the discrete IBCs (11) invokes two independent theoretical supports for the discretisation: by ensuring consistency as grid size $h \to 0$ we invoke the traditional support for finite differences; and by applying centre manifold theory based at $\gamma = 0$ we invoke the strong results of that theory for the holistic approximation at finite h. We expect such dual support to form powerful numerical approximations.

However, it is easy to imagine using the flexibility inherent in the introduction of the artificial IBCs in ways other than consistency. For example, we could try to

adapt the IBCs to generate the "flattest" centre manifold in some sense, thus hoping for small errors upon evaluation at $\gamma = 1$. This flexibility needs much more exploration.

6 Boundary conditions are straightforward

Recall that in Fig. 2 I showed a finite domain sliced into m elements. We applied artificial IBCs in between each element, either (5–6) or (11); this is adequate for strictly periodic problems as explored in [21]. Now we address how to incorporate the original physical boundary conditions at the extremes of the domain—for simplicity I only discuss the left end of the leftmost element, the right end is similar by symmetry.

The simplest case is that of a Neumann boundary condition of $u_x = a(t)$ at the left end $x = x_1 - h/2$. As explored in [20, §4], we may incorporate it by using

$$\frac{\partial v_1}{\partial x} = \gamma a(t) \quad \text{at} \quad x = x_1 - h/2 : \qquad (13)$$

when $\gamma = 0$ the leftmost element is insulated as required for the application of centre manifold theory (§4); whereas when $\gamma = 1$ the original Neumann boundary condition is recovered. The construction of the model then proceeds as before but with special treatment for those few elements near the boundary. We find, for example, that when keeping γ^2 terms, this boundary conditions affects the discretisation of the first two elements. For example, it introduces terms in the discretisation involving the not only the flux a, but also its time derivatives, $h^2\dot{a}$, $h^4\ddot{a}$, etc. The reason for these time derivatives is that the flux feeds into the subgrid scale fields of the boundary elements and so affects the interaction between the various physical processes. The scope for such interaction increases with increasing element size h and so accounts for the appearance of the h^2 factor in front of the time derivative $\dot{a}$. We need to know such effects on coarse grids.

As discussed in [20, §3] the best way to incorporate a Dirichlet boundary condition, $u = a(t)$, appears to be to apply it at a grid point $x = x_0 = x_1 - h$. With the discrete IBCs (11) we used

$$v_1(\boldsymbol{u}, x_0, \gamma) - v_1(\boldsymbol{u}, x_1, \gamma) = \gamma(a - u_1)\,, \qquad (14)$$

which is effectively insulating when $\gamma = 0$ and requires the Dirichlet condition is satisfied when $\gamma = 1$. The construction proceeds as before and the same qualitative observations apply as for Neumann boundary conditions. This centre manifold approach to discretisation provides a natural and unified method of determining approximations near a domain boundary.

7 Higher dimensional PDEs

So far we have only addressed PDEs in one spatial dimension. The same approach has the same theoretical support for constructing numerical models for dissipative PDEs in higher spatial dimensions. MacKenzie [11] is studying, for example, reaction-diffusion equations in two dimensions:

$$\frac{\partial u}{\partial t} = \nabla^2 u + \text{reaction}\,. \qquad (15)$$

The approach in [11] is to: tessellate space, by squares for example; apply IBCs analogous to either (5–6) or (11); invoke theory to support a model parametrised by the grid values of the field u; find the subgrid scale structures and the numerical model by iteratively solving Poisson's equation, $\nabla^2 v' = g' + \text{residual}$, in the elements. For the Liouville reaction-diffusion equation we find [11] the holistic model is more robust over a wider range of parameters.

In ongoing research into the construction of numerical models for the advection-diffusion in a channel or pipe, we find that the holistic discretisation automatically generates a model containing shear dispersion [26]. This is despite the analysis being for finite element size. We do not invoke large scale variations in the spread of material along the channel or pipe that hitherto has been necessary to derive shear dispersion.

8 Initial conditions are subtle

Now consider using a numerical model such as (4) to make a forecast. You have a given initial field $u_0(x)$, as shown schematically in Fig. 6, and are asked to use the numerical model to predict the field in the future. You might simply use the grid values of the given field, $u_j(0) = u_0(x_j)$, as the error would be at most $\mathcal{O}(h)$. However, in this approach the grid spacing h is treated as finite so such an error is significant. Instead, recall the Relevance theorem mentioned in §4: all small solutions of the PDE exponentially quickly evolve to solu-

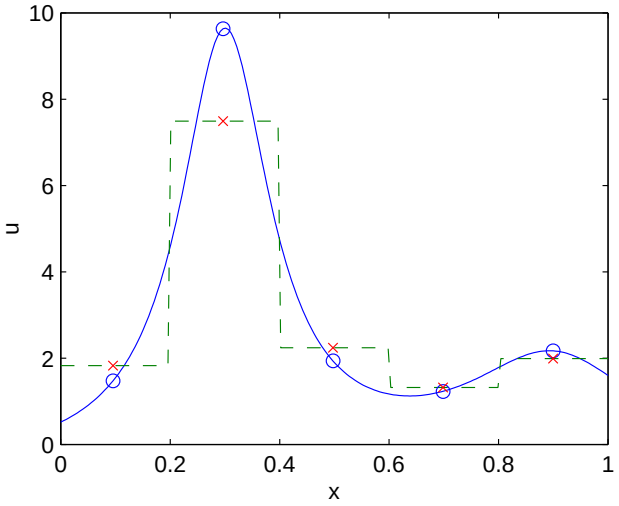

Figure 6: you are given an initial field (solid) in a domain divided into five elements, $h = 0.2$. The appropriate initial condition for the numerical model is *not* $u_0(x_j)$ (circles) as implied by the definition of u_j, *instead* use element averages (crosses) with $\mathcal{O}(\gamma)$ perturbations.

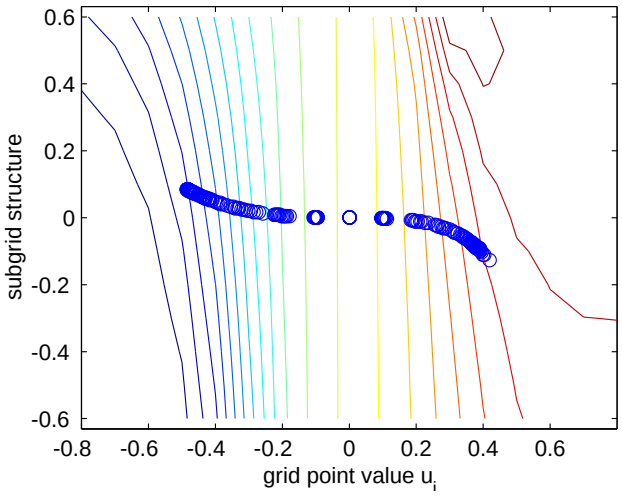

Figure 7: contours of solutions which have the same long term dynamics after exponential transients. The projection of initial conditions onto the centre manifold, symbolised by circles, is done along these contours.

tions of the model—see Fig. 4 for example. Remarkably, there is no mention of an error involving the grid spacing h! (Although recall the caveat that we have to use the model at $\gamma = 1$ which is not necessarily small.) Thus the issue is: given an initial field $u_0(x)$, what is the correct initial numerical grid values $u_j(0)$ to use to ensure the exponentially quick agreement assured by theory?

Consider the abstract view of the evolution shown in Fig. 4. The solutions from a wide variety of initial conditions exponentially quickly settled onto the centre manifold. All those that arrive at the same place at the same time on the centre manifold of the numerical model should be given the same initial condition. Thus we plot in Fig. 7 a contour plot of location on the centre manifold as a function of initial position: all solutions from any one contour have the same evolution apart from exponentially quickly decaying transients. Thus the initial condition problem is solved by projecting along the relevant contour onto the centre manifold and using the corresponding u_j as the initial condition for the model. Only then will the model solution and the PDE solution agree exponentially quickly.

The above geometric view of the projection of initial conditions was developed into an algebraic analysis invoking an adjoint differential equation [15, 3, 19]. See that the projection involves a dependence upon the initial subgrid fields so that the initial values for the numerical model are not simply the initial field evaluated at the grid points (sometimes called "initial slip" [9]). The projection for Burgers' equation (2) is given in [23]: it is a little involved but is the element average with $\mathcal{O}(\gamma)$ corrections. For example, for a point release in the kth element, $u_0(x) = \delta(x - x_k - h\eta)$, the dynamics of the linear diffusion equation [23, §3.1] requires the following slightly distributed initial condition for the numerical model:

$$\begin{aligned} hu_j(0) &= \left(\tfrac{7}{6} - \eta^2\right)\delta_{k,j} \\ &\quad + \left(-\tfrac{1}{12} - \tfrac{1}{2}\eta + \tfrac{1}{2}\eta^2\right)\delta_{k-1,j} \\ &\quad + \left(-\tfrac{1}{12} + \tfrac{1}{2}\eta + \tfrac{1}{2}\eta^2\right)\delta_{k+1,j}\,. \end{aligned} \quad (16)$$

This projection places most of the material in the kth element, but reasonably distributes some to the neighbouring elements depending upon where the material is released in the kth element.

9 Use the same paradigm

Recall the two layer model of the ocean, see Fig. 1. We now recognise it as the case of two finite elements

in the vertical with free surface boundary conditions above and below, and an artificial IBC in between the two layers. But further, for application to the broad ocean we need to describe the evolution of structures varying over large scales in the horizontal and how they interact with the flow in the two layers. Centre manifold theory has been invoked to model systematically fluid flows and continuum dynamics with large lateral extent [28, 17, 14, 25, e.g.]. Since the same dynamical system paradigm is used to construct numerical and analytical models it is straightforward to combine the two analyses.

For the two layer model of the ocean, in as yet unconcluded work, I have derived that the thickness and velocities in each layer evolve according to

$$\begin{aligned}
&\frac{\partial \eta_j}{\partial t} = -\boldsymbol{\nabla}\cdot(\eta_j \bar{\boldsymbol{u}}_j)\,,\\
&\frac{\partial \bar{\boldsymbol{u}}_1}{\partial t} = -\bar{\boldsymbol{u}}_1\cdot\boldsymbol{\nabla}\bar{\boldsymbol{u}}_1 + f\bar{\boldsymbol{u}}_1\times\boldsymbol{k} - \boldsymbol{\nabla}(\eta_1+\eta_2)\\
&-\frac{\eta_2}{3\eta_1}\boldsymbol{\nabla}\eta_1 - \frac{\rho''}{3}\left(1+\frac{2\eta_1 H}{15\nu_1}\right)\boldsymbol{\nabla}\eta_1\\
&+\frac{8H}{3\eta_1}(\bar{\boldsymbol{u}}_2-\bar{\boldsymbol{u}}_1) + \nu_1\nabla^2\bar{\boldsymbol{u}}_1 + 3\nu_1\boldsymbol{\nabla}(\boldsymbol{\nabla}\cdot\bar{\boldsymbol{u}}_1)\\
&+2\frac{\nu_1}{\eta_1}\boldsymbol{\nabla}\eta_1(\boldsymbol{\nabla}\cdot\bar{\boldsymbol{u}}_1) + 2\frac{\nu_1}{\eta_1}(\boldsymbol{\nabla}\eta_1\cdot\boldsymbol{\nabla})\bar{\boldsymbol{u}}_1\\
&+\frac{\nu_1}{\eta_1}\boldsymbol{\nabla}\eta_1\times(\boldsymbol{\nabla}\times\bar{\boldsymbol{u}}_1) - \frac{H\eta_2}{3\eta_1\nu_2}\boldsymbol{s}\,,
\end{aligned}$$

and similarly for $\partial\bar{\boldsymbol{u}}_2/\partial t$. Many terms are easily recognised, for example, conservation of material, advection, Corriolis force, hydrostatic pressure forcing, etc. Other terms arise through subtle interactions between physical processes. The centre manifold approach resolves such interactions.

10 Conclusion

In summary, this centre manifold approach to constructing numerical models of dissipative PDEs appears to have many advantages:

- it gives new theoretical support for a systematic discretisation at finite element size;
- in practise this comes from resolving subgrid scale structures and interactions between physical processes;
- boundary conditions are easily incorporated;
- it illuminates the initial conditions for accuracy; and
- the same modelling paradigm is used for both numerical and analytic models.

References:

[1] J. Carr. *Applications of centre manifold theory*, volume 35 of *Applied Math. Sci.* Springer-Verlag, 1981.

[2] J. Carr and R. G. Muncaster. The application of centre manifold theory to amplitude expansions. II. Infinite dimensional problems. *J. Diff. Eqns*, 50:280–288, 1983.

[3] S. M. Cox and A. J. Roberts. Initial conditions for models of dynamical systems. *Physica D*, 85:126–141, 1995.

[4] C. Foias, M. S. Jolly, I. G. Kevrekedis, G. R. Sell, and E. S. Titi. On the computation of inertial manifolds. *Phys Lett. A*, 131:433–436, 1988.

[5] C. Foias, M. S. Jolly, I. G. Kevrekidis, and E. S. Titi. Dissipativity of numerical schemes. *Nonlinearity*, 4:591–613, 1991.

[6] C. Foias, G. R. Sell, and E. S. Titi. Exponential tracking and approximation of inertial manifolds for dissipative nonlinear equations. *J. Dyn. & Diff. Eqns*, 1:199–244, 1989.

[7] C. Foias and E. S. Titi. Determining nodes, finite difference schemes and inertial manifolds. *Nonlinearity*, 4:135–153, 1991.

[8] B. Fornberg. On the instability of the leap-frog and Crank-Nicolson approximations of a nonlinear partial differential equation. *Maths of Comput.*, 27:45–57, 1973.

[9] F. Haake and M. Lewenstein. Adiabatic drag and intial slip in random processes. *Phys. Rev. A*, 28:3060–3612, 1983.

[10] D. A. Jones, L. G. Margolin, and E. S. Titi. On the effectiveness of the approximate inertial

manifold—a computational study. *Theoret. Comput. Fluid Dynamics*, 7:243–260, 1995.

[11] T. MacKenzie and A. J. Roberts. The dynamics of reaction diffusion equations lead to a holistic discretisation. In R. L. May, G. F. Fitz-Gerald, and I. H. Grundy, editors, *EMAC 2000 Proceedings. Proceedings of the fourth biennial Engineering Mathematics and Applications Conference*, pages 199–202, 2000.

[12] T. Mackenzie and A. J. Roberts. Holistic finite differences accurately model the dynamics of the Kuramoto-Sivashinsky equation. *ANZIAM J.*, 42(E):C918–C935, 2000. [Online] `http://anziamj.austms.org.au/V42/CTAC99/Mack`.

[13] M. Marion and R. Temam. Nonlinear Galerkin methods. *SIAM J. Numer. Anal.*, 26(5):1139–1157, 1989.

[14] R. V. N. Melnik, A. J. Roberts, and K. A. Thomas. Dynamics of shape-memory-alloys: A reduction procedure for 3d models. In W. Wunderlich, editor, *Proceedings of the European Conference on Computational Mechanics: Solids, Structures and Coupled Problems in Engineering*, page 328, 1999.

[15] A. J. Roberts. Appropriate initial conditions for asymptotic descriptions of the long term evolution of dynamical systems. *J. Austral. Math. Soc. B*, 31:48–75, 1989.

[16] A. J. Roberts. The utility of an invariant manifold description of the evolution of a dynamical system. *SIAM J. Math. Anal.*, 20:1447–1458, 1989.

[17] A. J. Roberts. Low-dimensional models of thin film fluid dynamics. *Phys. Letts. A*, 212:63–72, 1996.

[18] A. J. Roberts. Low-dimensional modelling of dynamics via computer algebra. *Comput. Phys. Comm.*, 100:215–230, 1997.

[19] A. J. Roberts. Computer algebra derives correct initial conditions for low-dimensional dynamical models. *Comput. Phys. Comm.*, 126(3):187–206, 2000.

[20] A. J. Roberts. Derive boundary conditions for holistic discretisations of burgers' equation. Technical report, [`http://arXiv.org/abs/math.NA/0106224`], 2001.

[21] A. J. Roberts. Holistic discretisation ensures fidelity to Burgers' equation. *Applied Numerical Modelling*, 37:371–396, 2001.

[22] A. J. Roberts. A holistic finite difference approach models linear dynamics consistently. *Mathematics of Computation*, to appear, 2001. [`http://arXiv.org/abs/math.NA/0003135`].

[23] A. J. Roberts. Holistic projection of initial conditions onto a finite difference approximation. *Computer Physics Communications*, to appear, 2001. [`http://arXiv.org/abs/math.NA/0101205`].

[24] J. C. Robinson. The asymptotic completeness of inertial manifolds. *Nonlinearity*, 9:1325–1340, 1996.

[25] S. A. Suslov and A. J. Roberts. Modelling of sample dynamics in rectangular asymmetrical flow field-flow fractionation channels. *Analytical Chemistry*, 72(18):4331–4345, 2000.

[26] G. I. Taylor. Conditions under which dispersion of a solute in a stream of solvent can be used to measure molecular diffusion. *Proc. Roy. Soc. Lond. A*, 225:473–477, 1954.

[27] R. Temam. Inertial manifolds. *Mathematical Intelligencer*, 12:68–74, 1990.

[28] S. D. Watt and A. J. Roberts. The accurate dynamic modelling of contaminant dispersion in channels. *SIAM J. Appl Math*, 55(4):1016–1038, 1995.